

Amino-functionalized pore-expanded SBA-15 for CO₂ adsorption

A. Olea · E. S. Sanz-Pérez · A. Arencibia ·
R. Sanz · G. Calleja

Received: 1 November 2012 / Accepted: 18 January 2013 / Published online: 30 January 2013
© Springer Science+Business Media New York 2013

Abstract The adsorption of CO₂ on pore-expanded SBA-15 mesostructured silica functionalized with amino groups was studied. The synthesis of conventional SBA-15 was modified to obtain pore-expanded materials, with pore diameters from 11 to 15 nm. Post-synthesis functionalization treatments were carried out by grafting with diethylenetriamine (DT) and by impregnation with tetraethylenepentamine (TEPA) and polyethyleneimine (PEI). The adsorbents were characterized by X-ray diffraction, N₂ adsorption–desorption at 77 K, elemental analysis and Transmission Electron Microscopy. CO₂ capture was studied by using a volumetric adsorption technique at 45 °C. Consecutive adsorption–desorption experiments were also conducted to check the cyclic behaviour of adsorbents in CO₂ capture. An improvement in CO₂ adsorption capacity and efficiency of amino groups was found for pore-expanded SBA-15 impregnated materials in comparison with their counterparts prepared from conventional SBA-15 with smaller pore size. PEI and TEPA-based adsorbents reached significant CO₂ uptakes at 45 °C and 1 bar (138 and 164 mg CO₂/g, respectively), with high amine efficiencies (0.33 and 0.37 mol CO₂/mol N), due to the positive effect of the larger pore diameter in the diffusion and accessibility of organic groups. Pore-expanded SBA-15 samples grafted with

DT and impregnated with PEI showed a good stability after several adsorption–desorption cycles of pure CO₂. PEI-impregnated adsorbent was tested in a fixed bed reactor with a diluted gas mixture containing 15 % CO₂, 5 % O₂, 80 % Ar and water (45 °C, 1 bar). A noteworthy adsorption capacity of 171 mg CO₂/g was obtained in these conditions, which simulate flue gas after the desulphurization step in a thermal power plant.

Keywords Pore-expanded SBA-15 · Amino-functionalization · Diethylenetriamine · Polyethyleneimine · Tetraethylenepentamine · CO₂ capture

1 Introduction

Carbon dioxide emissions are the most important anthropogenic contribution to the greenhouse effect, being originated by fossil fuel combustion. A lot of research effort has been done to develop renewable energies, as well as energy savings and efficiency programs. Additionally, carbon capture and storage (CCS) technologies are also considered as a suitable option to minimize greenhouse gas emissions from large CO₂ stationary sources (Metz et al. 2005), like thermal power stations or cement-production plants. Absorption processes using aqueous solutions of amines are widely used in CCS. However, these processes entail significant drawbacks, being the main problem the massive energy requirements for the amine regeneration (Tontiwachwuthikul et al. 1991; DOE 1999).

Gas-phase adsorption is considered as an efficient alternative to absorption technologies. It is based on the use of porous adsorbents such as zeolites, activated carbons, pillared clays, metal oxides or metal organic frameworks (Choi et al. 2009; Samanta et al. 2012). Physical adsorption

A. Olea · E. S. Sanz-Pérez
Department of Chemical and Environmental Technology,
ESCET. Universidad Rey Juan Carlos, C/ Tulipán s/n,
28933 Móstoles, Madrid, Spain
e-mail: eloy.sanz@urjc.es

A. Arencibia · R. Sanz · G. Calleja (✉)
Department of Chemical and Energy Technology, ESCET.
Universidad Rey Juan Carlos, C/ Tulipán s/n, 28933 Móstoles,
Madrid, Spain
e-mail: guillermo.calleja@urjc.es

is originated by weak intermolecular forces, most of them nonspecific interactions, present in all gas–solid systems (Barrer 1978). However, carbon dioxide molecule has a high quadrupolar moment and a subsequent high polarizability (Buckingham and Disch 1963), thus being selectively adsorbed when mixed with other gas molecules such as N_2 , O_2 , H_2 , Ar and CH_4 . Physisorption processes reach considerable uptakes at high pressure and low temperature, but flue gases from coal-fired thermal power stations after desulphurization typically present a low CO_2 concentration and are released at atmospheric pressure and temperatures around 45–55 °C (Gaikwad et al. 2003). In these conditions, chemical adsorption of CO_2 over hybrid organic–inorganic mesostructured materials becomes interesting due to their high adsorption capacity and selectivity. These adsorbents are prepared by incorporating organic functionalities to mesoporous supports, achieving high organic loadings. Regarding the organic functionalities, amino groups are commonly selected due to their selectivity towards CO_2 , forming ammonium carbamate under dry conditions (0.50 mol CO_2 /mol N) and ammonium carbonate or bicarbonate, depending on the pH, under wet atmosphere (1.0 mol CO_2 /mol N) (Caplow 1968). The CO_2 /N molar ratio parameter is often calculated, since it gives information about the efficiency of the reaction between CO_2 and amino groups.

The incorporation of amino groups in mesostructured materials can be accomplished by chemical or physical methods. Chemical procedures use organo-alcoxysilanes either by direct synthesis following the co-condensation method (Burkett et al. 1996, Macquarrie, 1996, Lim and Stein 1999, Stein et al. 2000) or by a post-synthesis reaction through the grafting route (Leal et al. 1995, Knowles et al. 2006, Harlick and Sayari 2007, Calleja et al. 2011). On the other hand, physical modification of porous materials is usually based on wet impregnation procedures, incorporating aminated molecules such as diethanolamine, DEA (Franchi et al. 2005), tetraethylenepentamine, TEPA (Yue et al. 2006) or even some polymers, like polyethyleneimine, PEI (Xu et al. 2002). The impregnation procedure yields higher nitrogen contents, although the adsorption kinetics and the adsorption efficiency of amino groups are usually lower than the corresponding to chemically modified materials.

With the aim of incorporating a higher amino content and simultaneously avoiding diffusion restrictions, the pore-expansion of mesostructured materials can offer an advantage. In fact, the functionalization by grafting of PE-MCM-41 with DT yielded a noticeable nitrogen content of 11 wt.% through a water-aided modified method (Harlick and Sayari 2007). This support was also impregnated with PEI, obtaining significant pure CO_2 adsorption capacities around 100 mg CO_2 /g at 50 °C and 1 bar (Heydari-Gorji et al. 2011).

In the present paper we have worked with pore-expanded SBA-15 materials that exhibit better properties compared with MCM-41. Some routes followed to obtain pore-expanded SBA-15 used linear alkanes as swelling agents (Sun et al. 2005), despite their low solubility in P123 micelles (Nagarajan et al. 1986, Nagarajan 1999). Other aromatic hydrocarbons such as 1,3,5-trimethylbenzene (TMB), 1,3,5-triethylbenzene and 1,3,5-triisopropylbenzene (TIPB), were also used. TMB has been frequently employed to obtain pore-expanded SBA-15, reaching pore diameters up to 300 Å (Zhao et al. 1998a, b), but the structure of the obtained material was foam-like instead of bidimensional (Lettow et al. 2000). TIPB has been satisfactorily used to obtain pore-expanded materials such as PE-MCM-41 (Namba and Mochizuki 1998) and PE-SBA-15 (Cao et al. 2009).

In this work, we have synthesised four pore-expanded SBA-15 silicas with noticeable higher pore diameters. PE-SBA-15 materials have been functionalized by grafting with diethylenetriamine (DT), and also by impregnation with PEI and tetraethylenepentamine. Pure CO_2 adsorption performance of the resulting materials was tested in a volumetric equipment, checking the influence of the higher pore diameter of PE-SBA-15 on the CO_2 adsorption. Besides, a series of adsorption–desorption experiments have been performed in a cyclic way to evaluate the stability of the most promising adsorbents in CO_2 capture. A fixed bed has also been used to check the adsorption from a gaseous mixture containing water.

2 Experimental section

2.1 Synthesis of SBA-15 mesostructured silica

SBA-15 conventional materials were prepared following the procedure reported by Zhao et al. (1998a). Pluronic P123 (PEO_{20} - PPO_{70} - PEO_{20} , $M_n \sim 5800$, Sigma-Aldrich) was used as a structure directing agent and TEOS (tetraethyl orthosilicate, 98 %, Sigma-Aldrich) as a silica source. Pluronic P123 was dissolved in 1.9 M HCl, stirring until complete dissolution. Then, TEOS was added to the previous mixture and a hydrolysis step at 40 °C for 20 h was carried out. The formation of the SBA-15 hexagonal mesostructure was completed by performing an ageing step at 110 °C for 24 h. The solid obtained was filtered and the surfactant was removed from the porous structure by calcining in air at 550 °C for 5 h or by ethanol-extraction for 24 h. Materials so obtained were named SBA-15c, and SBA-15e respectively (c: calcination; e: extraction).

Pore-expanded SBA-15 (PE-SBA-15) was prepared following the modified synthesis procedure reported by Cao et al. (2009), obtaining up to 40 g of PE-SBA-15.

Similarly to the synthesis of conventional SBA-15, Pluronic P123 was used as a structure directing agent and TEOS as a silica source. Besides, this procedure includes the use of TIPB (1,3,5-triisopropylbenzene, 96 %, Sigma-Aldrich) as a swelling agent and ammonium fluoride as a solubility enhancer. A P123:TIPB molar ratio of 2.4:1 was employed in order to preserve the mesoscopic structure while pore diameter is increased. Hydrolysis temperatures of 12 and 17 °C were used. The surfactant was removed from the mesostructure either by calcination in air at 550 °C for 5 h or by ethanol-extraction for 24 h. The resulting materials were named PE-SBA-15 (T_x), where T represents the hydrolysis temperature and x the method for surfactant removal (c: calcination; e: extraction).

2.2 Functionalization of SBA-15

2.2.1 Grafting

PE-SBA-15 materials were functionalized by grafting with diethylenetriamine-trimethoxysilane, (DT, Sigma-Aldrich), according to the procedure described elsewhere (Leal et al. 1995). A DT/silica ratio of 1.83 (wt.) was used, corresponding to the complete coverage of a hypothetical surface silanol concentration of 6 SiOH/nm² on pore walls (Calleja et al. 2011). The resulting materials were dried at room temperature overnight according to previous results, since air-drying of amino-grafted solids at higher temperatures (110 °C) was found to degrade the amino groups, yielding groups with no reactivity towards CO₂ (Calleja et al. 2011). The functionalized materials were named PE-SBA-15-(T_x)-DT.

2.2.2 Impregnation

PEI (branched polyethyleneimine, average molecular weight 800, $\rho = 1.05$ g/mL) and TEPA ($\rho = 0.998$ g/mL), both from Sigma-Aldrich, were used to functionalize ethanol-extracted PE-SBA-15 (17e) by wet impregnation. A 50 wt.% PEI or TEPA was used to obtain impregnated adsorbents by using methanol as a solvent and a methanol/silica weight ratio of 8 (Xu et al. 2002). The resulting solids were dried at room temperature overnight, being named PE-SBA-15 (17e)-PEI and PE-SBA-15 (17e)-TEPA, respectively.

2.3 Characterization

2.3.1 Physico-chemical characterization

Siliceous and functionalized materials were characterized by low angle X-Ray diffraction with a powder diffractometer PHILIPS X-PERT MPD using the CuK α monochromatic

radiation. Transmission electron micrographs were acquired on a Phillips Tecnai 20 electronic microscope working at 200 kV.

Nitrogen adsorption-desorption isotherms at 77 K were measured using a Micromeritics Tristar-3000 sorptometer. Samples were outgassed in N₂ flow for 8 h at 200 and 150 °C for original siliceous and functionalized samples respectively. Specific surface area was determined with the B.E.T. equation (P/P_0 between 0.05 and 0.20), pore size distribution was determined by applying the B.J.H. model (assuming cylindrical pore geometry) to the adsorption branch of the isotherm, and total pore volume was obtained at $P/P_0 \geq 0.97$ (Sing et al. 1985). Nitrogen content was determined by elemental analysis in a Vario EL III Elemental Analyzer System GMHB.

2.3.2 Adsorption of CO₂

Pure CO₂ adsorption-desorption isotherms were obtained in a VTI Scientific Instruments HVPA-100 equipment, at 45 °C and pressures in the range 0–6 bar. Samples were outgassed at 110 °C for 2 h under vacuum (5×10^{-3} mbar). Free volume was determined by helium measurements prior to the obtention of each isotherm. Sievert method was used to determine the free volume and to acquire isotherm points. Two alternative criteria were considered for adsorption equilibrium: a maximum equilibration time of 60 min or a pressure drop below 0.2 mbar/3 min.

Cyclic CO₂ adsorption/desorption tests of pure CO₂ at 1 bar were performed in a DSC-TGA thermobalance model SDT Simultaneous 2960 from TA instruments. A regeneration step at 110 °C for 2 h was performed after each cycle. Equilibration time for adsorption was 3 h, while for desorption was only 1 h, time enough to achieve a complete CO₂ desorption at 110 °C.

The influence of CO₂ dilution and the presence of water in the initial mixture were studied by carrying out CO₂ adsorption experiments in a fixed bed (PID Eng & Tech Microactivity-Reference, 0.91 cm inner diameter, 10 cm length) coupled to a mass spectrometer (Pfeiffer Vacuum QMG220). The gas stream was fed to the fixed bed at atmospheric pressure and 45 °C, having the following dry composition: 15 % CO₂, 5 % O₂, 80 % Ar, and a water content of 5 wt.%. Adsorbent samples (500 mg) were outgassed previously to every adsorption run, using an Ar stream flow (100 mL/min) at 110 °C, being enough with an outgassing time of 2 h. After that, the temperature was decreased to 45 °C and subsequently, the gas mixture was introduced. The CO₂ adsorbed volume was calculated by integrating the resulting breakthrough curves (q_{CO_2} vs. time).

3 Results and discussion

3.1 Pore-expanded SBA-15 materials

Pore-expanded SBA-15 materials have been obtained by modifying the conventional synthesis (Zhao et al. 1998a) with the addition of a swelling agent (TIPB) and a solubility enhancer (NH_4F), and the decrease of the hydrolysis temperature to 12 and 17 °C (Cao et al. 2009).

Figure 1 shows the low angle X-ray diffractograms of pore-expanded SBA-15 materials compared to conventional SBA-15 supports. Calcined (Fig. 1a) and ethanol-extracted (Fig. 1b) supports exhibit diffraction peaks characteristic of a hexagonal bidimensional structure. However X-ray diffraction peaks for pore-expanded materials show a shift to lower angles, due to the larger cell parameters (a_0) of these materials (13.9–16.3 nm) compared to conventional SBA-15 supports (12.0 nm). These data are shown in Table 1. Regarding the intensity of diffraction peaks, it is lower for PE-SBA-15 than for conventional SBA-15 materials, likely due to a slight loss of the mesostructure during the pore-expansion process. This behaviour is more pronounced for samples synthesised at 12 °C, since this temperature is closer to the Krafft point or critical micelle temperature, which is around 10 °C for similar systems (Fan et al. 2005).

Figure 2 displays the nitrogen adsorption–desorption isotherms at 77 K for SBA-15 and PE-SBA-15 materials and Table 1 shows their textural properties. A clear difference is observed for pore-expanded materials, as the capillary condensation in mesopores occurs at a higher relative pressure, due to their larger pore diameter compared to conventional SBA-15. Pore diameter values found for conventional ethanol-extracted and calcined SBA-15 are 8.2 and 9.0 nm, respectively, and 11.3–15.2 nm for pore-expanded materials. It should be noted that this significant increase in the pore diameter above 12.0 nm obtained with the procedure by Cao et al. (2009), exceeds the highest value achieved with TMB (1,3,5-trimethylbenzene) without losing the mesostructured order.

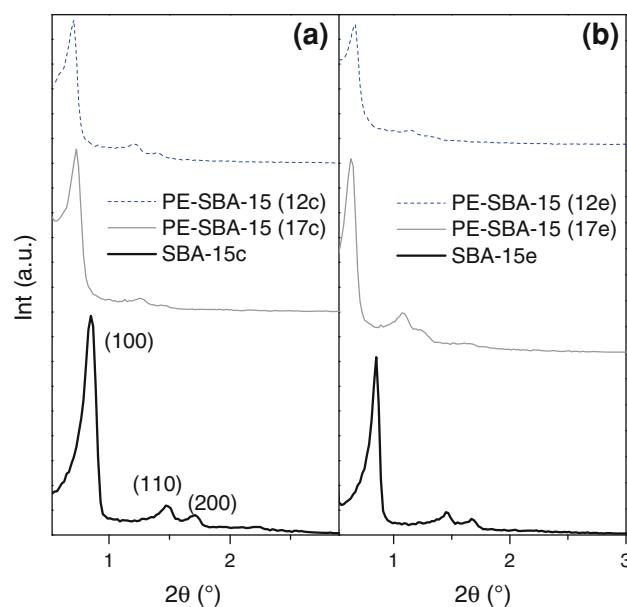


Fig. 1 Low angle X-ray diffractograms for conventional SBA-15 silica and pore-expanded SBA-15 materials obtained by **a** calcination and **b** ethanol extraction

Attempts to obtain larger values of the pore diameter by using TMB resulted in a phase change, obtaining foam-like structures (Lettow et al. 2000).

The main difference observed between materials prepared at 12 and 17 °C is the resulting total pore volume. Samples prepared at 17 °C achieve pore volumes around 1 cm^3/g , similar to values of conventional SBA-15, and significantly higher than the observed for pore-expanded supports prepared at 12 °C (0.80–0.85 cm^3/g). Besides, a higher nitrogen uptake at relative pressures above 0.9 is observed for materials prepared at 17 °C. This increased adsorption is related to the interparticle spaces of around 70 nm, the B.J.H. method offering an accurate estimation of interparticle porosity (Haynes 1975).

The procedure of surfactant removal is also playing a significant role. Thus, calcination at 550 °C entails a certain structure shrink, yielding materials with lower pore diameter and lower pore volume in comparison with

Table 1 Textural properties and pure CO_2 uptake (adsorption branch, 45 °C, 1 bar) of conventional SBA-15 and modified pore-expanded materials

Adsorbent	a_0 (nm)	S_{BET} (m^2/g)	D_{PORE} (nm)	V_{PORE} (cm^3/g)	HC ^a (wt.%)	CO_2 adsorption capacity (mg CO_2/g sample)
SBA-15c	12.1	692	9.0	1.03	–	21.8
PE-SBA-15 (17c)	13.9	452	11.7	1.02	–	15.7
PE-SBA-15 (12c)	14.7	437	11.3	0.80	–	11.5
SBA-15e	12.0	599	8.2	1.09	8.7	12.5
PE-SBA-15 (17e)	16.3	428	15.2	1.18	6.6	11.7
PE-SBA-15 (12e)	15.3	399	12.1	0.85	6.5	11.6

^a Organic content measured by elemental analysis

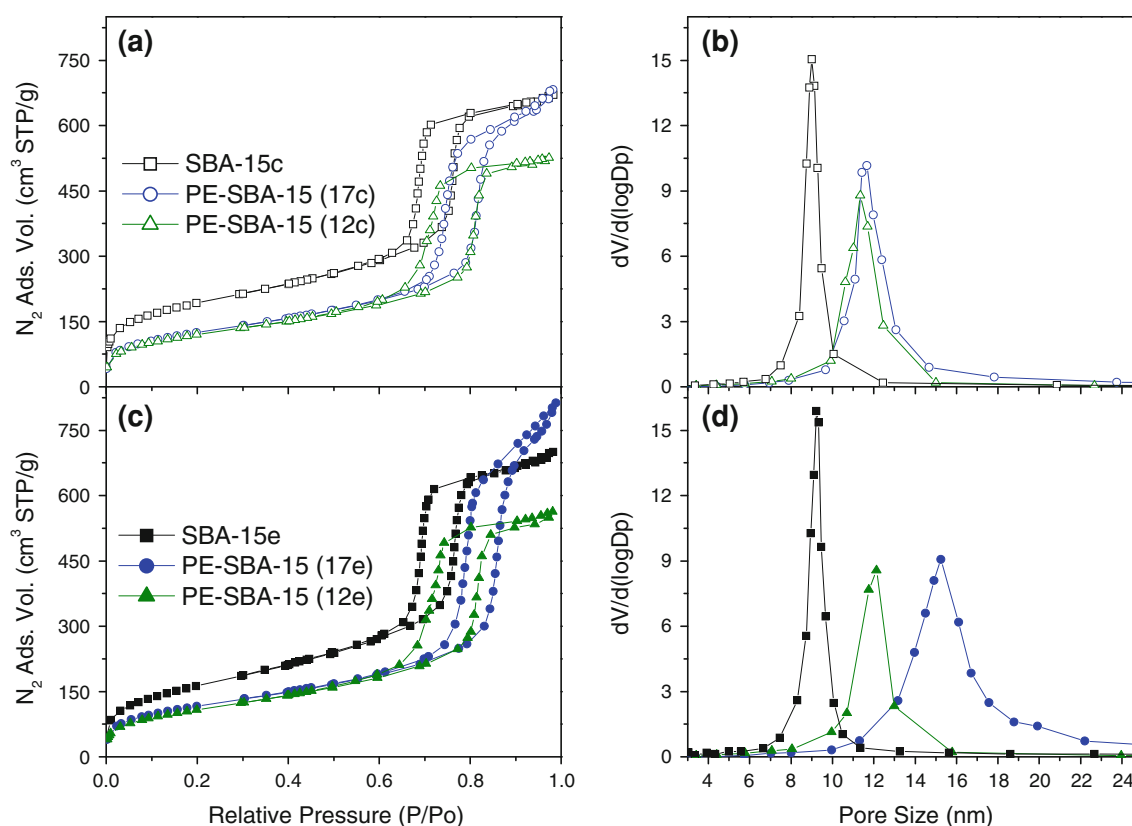


Fig. 2 Nitrogen adsorption–desorption isotherms at 77 K and BJH pore size distributions for conventional SBA 15 and pore-expanded SBA-15 materials calcined **a, b** and ethanol-extracted **c, d**

extracted supports. However, the calcination method produces a complete removal of the surfactant, while extracted supports present a remaining organic amount between 6.5 and 8.7 %. Calcined materials achieve also a higher surface due to the better removal of the surfactant.

Finally, the hydrolysis temperature influences the pore diameter of the resulting materials, as PE-SBA-15 supports prepared at 17 °C achieve pore diameter values of 11.7 nm (calcined) and 15.2 nm (extracted), while the hydrolysis at 12 °C produces materials with lower pore diameters (11.3 and 12.1 nm, respectively). The explanation of this difference is that 12 °C is a temperature too close to the Krafft point, as previously mentioned, being the resulting structures probably less ordered than their counterparts at 17 °C (Fan et al. 2005).

Surface area values for pore-expanded materials prepared at 17 °C are higher (428 and 452 m²/g) than those achieved at 12 °C (399 and 437 m²/g), being not far from surface area values of SBA-15 conventional supports (599 and 629 m²/g).

Figure 3 shows the transmission electron micrographs of SBA-15c and PE-SBA-15 (17e) materials. As seen, the pore-expanded support (Fig. 3c, d) presents smaller and more fragmented particles than conventional SBA-15c

(Fig. 3a, b). This fact could explain the higher nitrogen uptake observed at the highest relative pressures, associated to the interparticle adsorption.

Figure 4 presents pure CO₂ adsorption–desorption isotherms at 45 °C for pore-expanded materials. As seen, the isotherms of conventional SBA-15 supports show the same three characteristics: a negligible CO₂ uptake at low partial pressures, a continuous increase of CO₂ uptake with pressure and the reversibility of the process, as shown by the overlapping of the adsorption and desorption branches of the isotherms. These features are characteristic of physical adsorption, where weak adsorbent–adsorbate interactions determine the adsorption properties. Pore-expanded materials present similar CO₂ adsorption values at 1 bar, ranging from 5 to 15.7 mg CO₂/g. Their CO₂ uptakes are lower than the observed for conventional SBA-15, probably due to the smaller value of surface area, being this effect more pronounced at higher pressures.

3.2 Grafting of pore-expanded SBA-15

In a further step all PE-SBA-15 materials were functionalized by grafting with DT. N₂ adsorption–desorption isotherms at 77 K of the functionalized samples can be

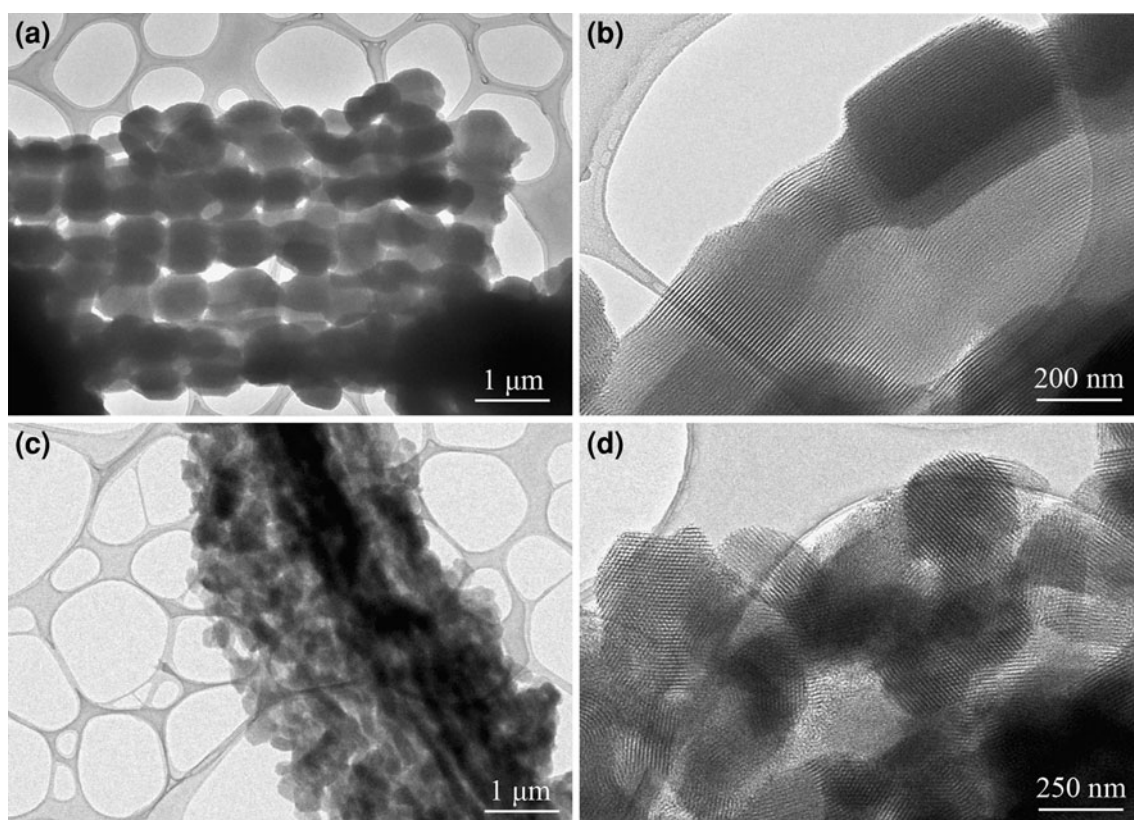


Fig. 3 TEM micrographs of **a, b** SBA-15c conventional silica and **c, d** pore-expanded PE-SBA-15 (17e) material

observed in Figure 5 along with those corresponding to the pure siliceous materials. A reduction in nitrogen adsorption was produced as a result of functionalization, which is related to the presence of organosilane molecules within the pores. Functionalized materials prepared at 17 °C yielded a reduction in their textural properties, and a further decrease was observed for functionalized materials prepared at 12 °C. Their respective BET surface area, pore diameter and pore volume values are shown in Table 2.

The method of surfactant removal seems again to be a very significant variable in the extension of the grafting process. In general, the amount of amino-containing molecules incorporated to the ethanol-extracted materials is higher than the corresponding to the calcined ones. Thus, nitrogen contents listed in Table 2 show that the organic incorporation is higher for extracted supports (7.8 and 8.6 % N for PE-SBA-15-(17e)-DT and PE-SBA-15-(12e)-DT, respectively) than for calcined materials (6.5 and 6.4 %

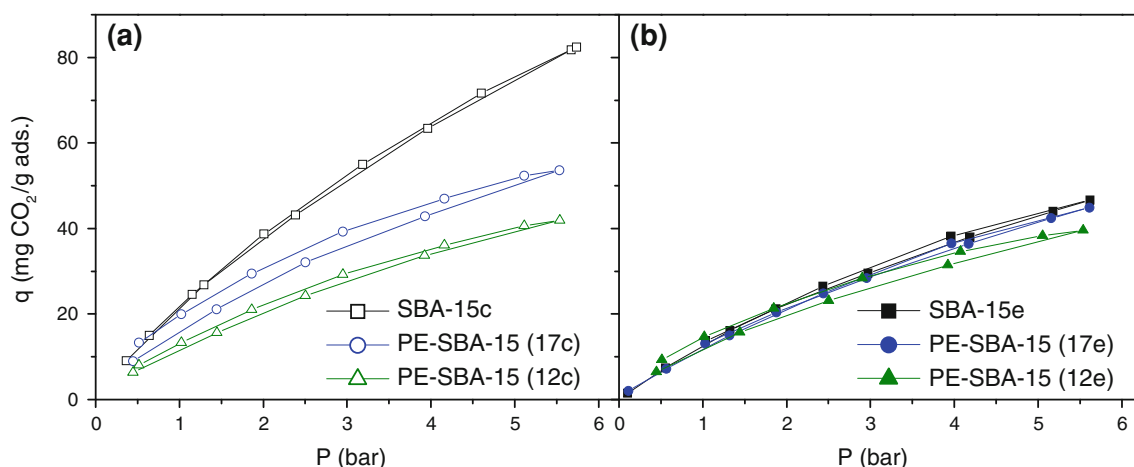


Fig. 4 CO₂ adsorption–desorption isotherms at 45 °C for conventional SBA-15 silica and pore-expanded SBA-15 materials obtained by **a** calcination and **b** ethanol extraction

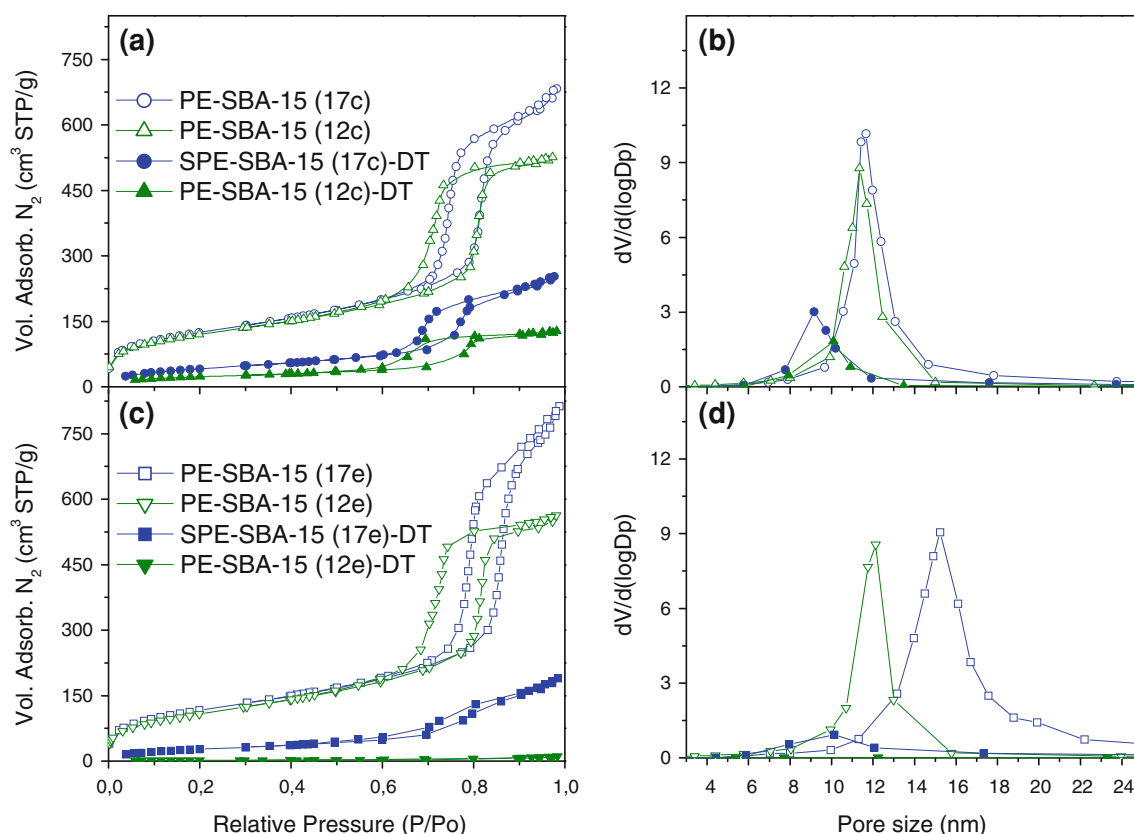


Fig. 5 **a, c** Nitrogen adsorption–desorption isotherms at 77 K and **b, d** BJH pore size distributions of pore-expanded SBA-15 silicas before and after grafting with DT

for PE-SBA-15-(17c)-DT and PE-SBA-15-(12c)-DT, respectively). These differences are probably due to the higher silanol surface concentration of the extracted material, as this parameter depends on the thermal history of the silica support, being estimated in 1.7 SiOH/nm^2 for samples calcined at 550°C , and in 5 SiOH/nm^2 for ethanol-extracted supports (van der Voort et al. 1991).

Conventional SBA-15 silicas present nitrogen contents that are higher for calcined and lower for extracted samples (7.3 % for SBA-15c-DT and 6.7 % for SBA-15e-DT, Calleja et al. 2011) than their pore-expanded counterparts, showing that pore expanding favours the grafting process only for extracted materials.

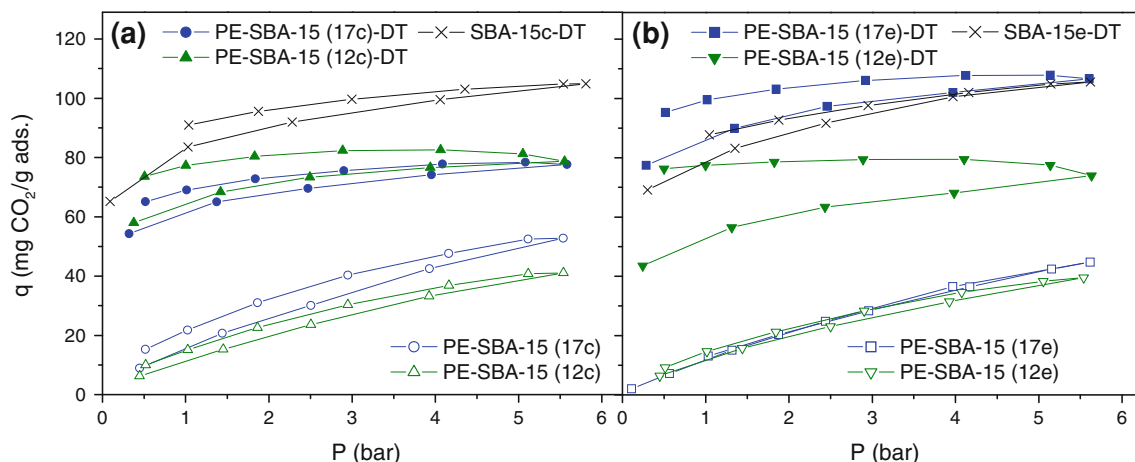
Pure CO_2 adsorption–desorption isotherms at 45°C for conventional and pore-expanded grafted materials are displayed in Figure 6. Functionalized adsorbents show different trends in their CO_2 adsorption isotherms compared to non-functionalized siliceous supports, as previously observed (Calleja et al. 2011; Sanz et al. 2012). Grafted supports present quite a high CO_2 uptake at very low partial pressure but then the uptake increase at higher pressures is lower than the observed for siliceous materials. The changes observed in comparison with the typical tendency of physical adsorption described for

siliceous supports are due to the contribution of chemical adsorption, which is produced by the presence of amino groups in the grafted materials. Another difference is that the adsorption and desorption branches do not entirely overlap in functionalized materials, since CO_2 chemisorption is not completely reversible at the adsorption temperature, 45°C . Some samples with a high organic content even experience a slight increase in the desorption branch of their isotherms. This fact may be related to a diffusion resistance of CO_2 through filled pores that avoids the achievement of a strict equilibrium in the adsorption branch.

Table 2 lists CO_2 adsorption capacities ($\text{mg CO}_2/\text{g}$) and efficiencies ($\text{mol CO}_2/\text{mol N}$) at 45°C and 1 bar for grafted adsorbents. Functionalized pore-expanded samples obtained by calcination, PE-SBA-15-(17c)-DT and PE-SBA-15-(12c)-DT, achieved similar CO_2 uptakes (61.2 and $64.2 \text{ mg CO}_2/\text{g}$, respectively), showing also similar nitrogen contents (6.5 and 6.4 %N) and amine efficiencies (0.30 and $0.32 \text{ mol CO}_2/\text{mol N}$). Comparatively, the grafting of conventional SBA-15 yielded SBA-15c-DT, with a nitrogen content of 7.3 %, achieving a higher CO_2 adsorption capacity ($82.0 \text{ mg CO}_2/\text{g}$) and a higher efficiency ($0.36 \text{ mol CO}_2/\text{mol N}$) in the same conditions.

Table 2 Textural properties, nitrogen content and pure CO₂ uptake (adsorption branch, 45 °C, 1 bar) of conventional and pore-expanded SBA-15 materials functionalized by grafting with DT

Adsorbent	S _{BET} (m ² /g)	D _p (nm)	V _p (cm ³ /g)	N (wt.%)	CO ₂ adsorption capacity	
					mg CO ₂ /g sample	mol CO ₂ /mol N
SBA-15c-DT	166	5.8	0.30	7.3	82.0	0.36
PE-SBA-15 (17c)-DT	158	9.2	0.38	6.5	61.2	0.30
PE-SBA-15 (12c)-DT	86	10.1	0.19	6.4	64.2	0.32
SBA-15e-DT	207	7.2	0.46	6.7	78.4	0.37
PE-SBA-15 (17e)-DT	104	10.1	0.28	7.8	85.8	0.35
PE-SBA-15 (12e)-DT	8	7.7	0.02	8.6	52.0	0.19

**Fig. 6** CO₂ adsorption–desorption isotherms at 45 °C for conventional SBA-15 silica and pore-expanded materials obtained by **a** calcination and **b** ethanol extraction

Functionalized pore-expanded samples obtained by extraction, PE-SBA-15-(17e)-DT and PE-SBA-15-(12e)-DT, reached a higher nitrogen content (7.8 and 8.6 % N, respectively) than their calcined counterparts. Accordingly, PE-SBA-15-(17e)-DT presents a better CO₂ adsorption capacity an amine efficiency (85.8 mg CO₂/g and 0.35 mol CO₂/mol N, respectively) than PE-SBA-15-(17c)-DT, which is the result of a higher density of tethered amines (Aziz et al. 2012). These values of CO₂ uptake and amine efficiency are similar to those obtained by grafted conventional SBA-15, as shown in Fig. 6 and Table 2.

CO₂ adsorption uptake and efficiency for PE-SBA-15-(12e)-DT are smaller than for the rest of materials, in spite of having the highest nitrogen content (8.6 % N). This behaviour is due to the organic overloading during the grafting process, saturating the pores and hindering CO₂ diffusion towards inner amino sites.

3.3 Impregnation of pore-expanded supports

Taking into account the results obtained with grafted samples, the siliceous material PE-SBA-15-(17e) has been selected as the best support to be further functionalized by

impregnation with PEI and TEPA. Figure 7 presents nitrogen adsorption–desorption isotherms at 77 K for PE-SBA-15 (17e) sample impregnated with 50 % PEI and with 50 % TEPA. As seen, these samples yielded a lower nitrogen adsorption, due to the pore filling with the aminated compounds, as observed in their textural properties (Table 3). A more pronounced reduction in the textural properties is observed for PEI-impregnated samples compared to TEPA-containing materials, due to the higher viscosity of PEI and its subsequent difficulty for pore diffusion during the impregnation process. For this reason, partial pore occlusion and PEI polymer deposition on the external surface could occur during the impregnation of PEI-functionalized materials, having both effects a negative influence on gas diffusion through the porous system of the impregnated structure (Sanz et al. 2012).

Nitrogen content of impregnated materials was 14.1 % for PE-SBA-15 (17e)-TEPA and 13.2 % PE-SBA-15 (17e)-PEI (Table 3). These values represent a considerable increase compared to grafted samples (6.4–7.8 %), but are similar to those obtained by the impregnation of conventional SBA-15 (Sanz et al. 2010), as this functionalization procedure is not restricted by surface area or the

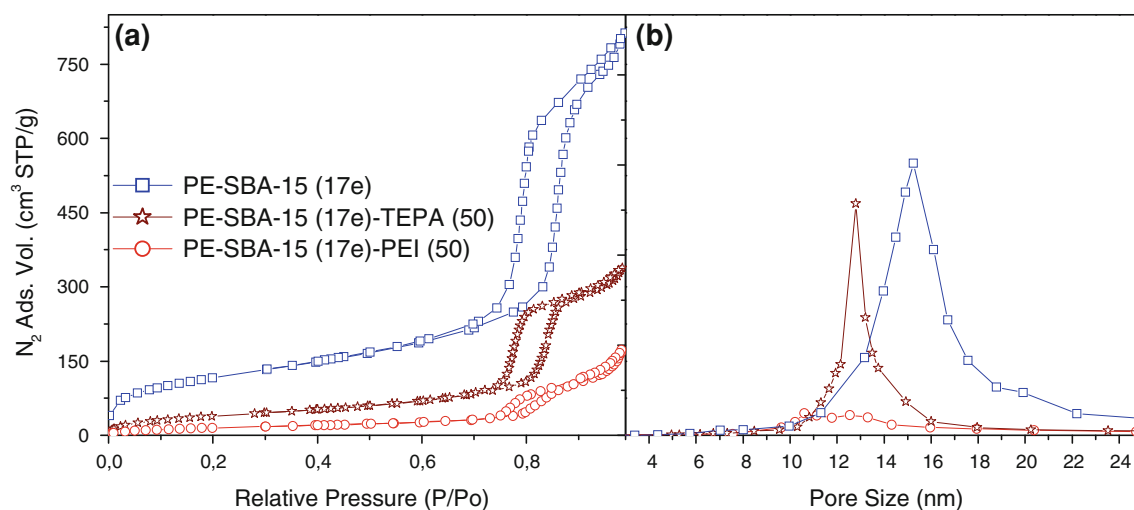


Fig. 7 **a** Nitrogen adsorption–desorption isotherms at 77 K and **b** BJH pore size distributions of PE-SBA-15 (17e) siliceous material and samples functionalized with TEPA and PEI

Table 3 Textural properties, nitrogen content and pure CO₂ uptake (adsorption branch, 45 °C, 1 bar) of PE-SBA-15 (17e) pore-expanded support functionalized by impregnation with PEI and TEPA

Adsorbent	S _{BET} (m ² /g)	D _p (nm)	V _p (cm ³ /g)	N (wt.%)	CO ₂ adsorption capacity	
					mg CO ₂ /g sample	mol CO ₂ /mol N
PE-SBA-15 (17e)	428	15.2	1.18	0.2	11.7	–
PE-SBA-15 (17e)-TEPA	150	12.8	0.49	14.1	164	0.37
PE-SBA-15 (17e)-PEI	59	10.6	0.22	13.2	138	0.33

available silanol groups. Nevertheless, some parameters such as the total pore volume are relevant for the CO₂ adsorption properties, as will be discussed later.

Figure 8 shows pure CO₂ adsorption–desorption isotherms at 45 °C and pressures ranging from 0 to 6 bar. These isotherms present a high CO₂ adsorption capacity at low pressures, reaching values very close to the uptakes at 6 bar (almost 200 mg CO₂/g), so that a very little dependence of the CO₂ adsorption with pressure is observed. Also, the desorption branch of these isotherms is almost horizontal, thus showing a virtually complete irreversibility of the adsorption process at 45 °C. These isotherms illustrate an extreme case of the aforementioned characteristic features of chemical adsorption. The explanation of this behaviour is related to the high nitrogen content of impregnated samples (13.2–14.1 %) and to the high efficiency of the amino groups in the CO₂ adsorption process (0.33 and 0.37 mol CO₂/mol N), that yields adsorption capacities of 138 and 164 mg CO₂/g at 45 °C and 1 bar for PE-SBA-15-PEI and PE-SBA-15-TEPA, respectively. These efficiency values are noteworthy, since the maximum value under dry conditions is 0.50 mol CO₂/mol N. When conventional SBA-15 was impregnated with a

similar amount of TEPA and PEI, adsorption capacities of 80.8 and 99.8 mg CO₂/g were obtained, while efficiency values were as low as 0.19 and 0.21 mol CO₂/mol N, respectively (Sanz et al. 2010).

As seen, the adsorption of CO₂ over pore-expanded SBA-15 supports seems to be favoured by the larger size of the pore diameter of the host material, very likely due to the better distribution and higher mobility of the organic amine molecules and the better diffusion of CO₂ through the filled pores. A similar finding was described by Ahn and co-workers for several mesostructured materials with pore diameters ranging 2.8–6.5 nm (Son et al. 2008).

With the aim of comparing the CO₂ adsorption results of this study with other found in the literature, Table 4 lists pure CO₂ uptake values at 45–50 °C and 1 bar of several mesostructured silicas impregnated with ca. 50 % PEI. CO₂ adsorption capacities of PEI-impregnated supports such as MCM-41 (Xu et al. 2002), HMS (Chen et al. 2010), SBA-15 (Sanz et al. 2010) and KIT-6 (Son et al. 2008) are presented, showing values in the range 44–110 mg CO₂/g. Pore-expanded MCM-41 has also been impregnated with PEI after calcination or ethanol-extraction, achieving capacities of 61 and 108 mg CO₂/g respectively (Harlick and Sayari 2007).

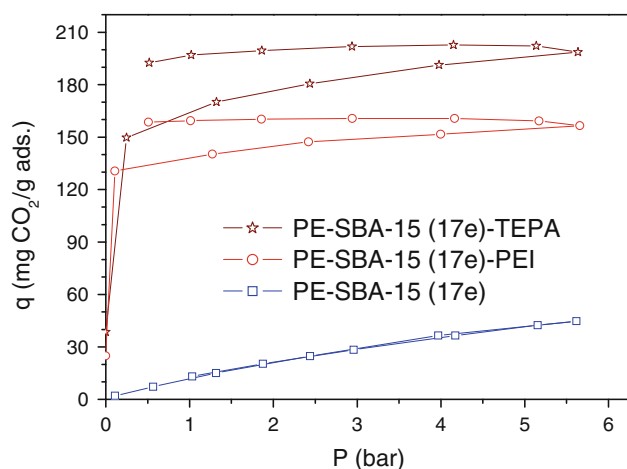


Fig. 8 CO₂ adsorption–desorption isotherms at 45 °C of PE-SBA-15 (17e) mesostructured silica and adsorbents obtained by impregnation with TEPA and PEI

Since the PEI content of these materials ranges 45–55 %, efficiency ratios for these samples are between 0.11 and 0.26 mol CO₂/mol N.

From this comparison it is concluded that the highest net CO₂ uptakes and adsorption efficiency values are obtained by PE-SBA-15 (17e)-PEI, reaching values of 138 mg CO₂/g and 0.33 mol CO₂/mol N.

3.4 Regeneration study and influence of the CO₂ dilution

Three selected samples, PE-SBA-15 (17e)-DT, PE-SBA-15 (17e)-PEI and PE-SBA-15 (17e)-TEPA, were tested in a thermobalance equipment to check their behaviour in cyclic experiments. Up to four CO₂ adsorption–desorption cycles were performed at 45 °C and 1 bar with each adsorbent. Despite the irreversibility of the chemisorption process in the adsorption conditions (45 °C), these materials can be easily regenerated by increasing the temperature. Thus, a temperature of 110 °C was used for regeneration, maintaining each material at this temperature for 2 h under nitrogen flow after each adsorption–desorption cycle. Figure 9 shows the results, being the adsorption

capacity for each cycle expressed relative to the first cycle uptake. As seen, CO₂ adsorption capacity for DT-grafted and PEI-impregnated samples is maintained after 4 cycles, as usually described for similar materials (Xu et al. 2002). However, TEPA-impregnated adsorbent undergoes a steady loss of adsorption capacity along the four cycles, possibly due to a partial evaporation of the TEPA or even to a degradation of this compound. This behaviour of TEPA impregnated materials has been also reported for similar adsorbents (Yue et al. 2006). Final uptake at the fourth cycle is equivalent to the 74 % of the initial CO₂ adsorption capacity (first cycle), which still represents a considerable net uptake of 105 mg CO₂/g. These results indicate that prepared materials could be potentially used as adsorbents at industrial scale for CO₂ capture by using TSA (temperature swing adsorption) and VSA (vacuum swing adsorption) techniques.

Finally, an additional experiment was performed in a fixed bed reactor with a diluted gas mixture containing 15 % CO₂, 5 % O₂, 80 % Ar (dry basis) and a mass water content of 5 % at a total pressure of 1 bar. The sample selected for this experiment was PE-SBA-15 (17e)-PEI. Exit gas stream of the fixed-bed reactor was analyzed with a mass spectrometer. The breakthrough curve corresponding to CO₂ is shown in Fig. 10, along with the integral equation used to obtain the CO₂ mass uptake. This value resulted 171 mg CO₂/g, which represents an increase of 24 % with respect to the adsorption capacity of pure CO₂ in anhydrous conditions at the same temperature. This increase is assigned to a change of the CO₂ adsorption mechanism in wet conditions, where the 1:2 CO₂/NH stoichiometry is changed to 1:1 due to the presence of moisture (Caplow 1968). Similar increases have been observed with other impregnated materials (Chen et al. 2009).

4 Conclusions

Four pore-expanded SBA-15 mesostructured silicas have been synthesized. Pore-expanded PE-SBA-15 mesostructured materials showed a significant pore-diameter

Table 4 Pure CO₂ uptake at 45–50 °C and 1 bar of siliceous mesostructured materials functionalized with around 50 % PEI

Adsorbent	T _{ads} (°C)	CO ₂ adsorption (mg CO ₂ /g sample)	Ref.
MCM-41-PEI-50	50	44	Xu et al. (2002)
45PEI/HMS-C	50	53	Chen et al. (2010)
PMC-PEI(55) ^a	50	61	Harlick and Sayari (2007)
SBA-15-PEI (50)	45	81	Sanz et al. (2010)
KIT-6-PEI-50	50	95	Son et al. (2008)
PME-PEI (55) ^a	50	108	Harlick and Sayari (2007)
PE-SBA-15 (17e)-PEI	45	138	Present work

^a PMC and PME stand for PE-MCM-41 calcined and ethanol-extracted respectively

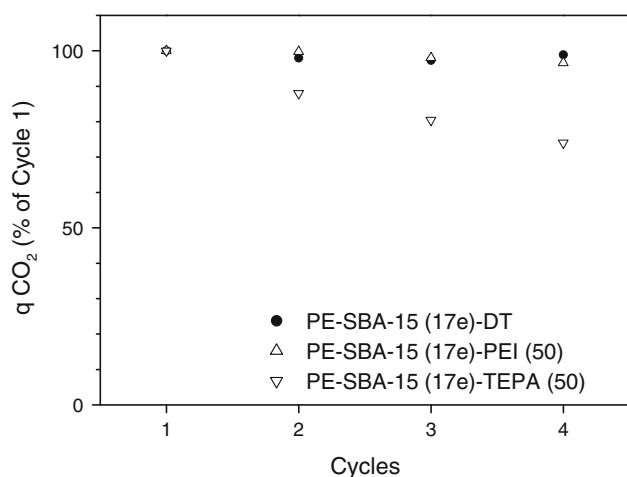


Fig. 9 Cyclic adsorption-desorption behaviour of CO₂ adsorbents synthesised by grafting and impregnation of PE-SBA-15 (17e) mesostructured silica

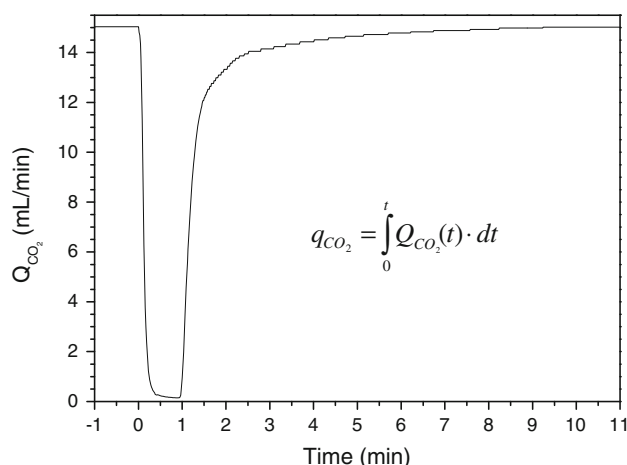


Fig. 10 Breakthrough curve of CO₂ for gas adsorption with PE-SBA-15 (17e)-PEI using a feed gas mixture containing 15 % CO₂, 5 % O₂, 80 % Ar (dry basis) and a mass water content of 5 % (1 bar, 45 °C)

increase, more pronounced for materials prepared using a hydrolysis temperature of 17 °C and surfactant removal by ethanol-extraction.

PE-SBA-15 supports have been functionalized by grafting with DT, yielding a higher amino group incorporation compared to conventional SBA-15 materials, as a result of the higher pore diameter. Sample PE-SBA-15 (17e)-DT showed the best results, reaching a high capture efficiency at 1 bar and 45 °C (0.35 mol CO₂/mol N), that led to a CO₂ adsorption uptake of 85.8 mg CO₂/g.

PE-SBA-15 (17e) was further functionalized by impregnation with PEI and TEPA, obtaining nitrogen contents higher than those achieved by grafted samples. PE-SBA-15 (17e)-PEI and PE-SBA-15 (17e)-TEPA materials attained considerable CO₂ uptakes at 1 bar (138 and

164 mg CO₂/g), with also high capture efficiencies (0.33 and 0.37 mol CO₂/mol N). These values are significantly higher than those of conventional SBA-15, which is the result of the higher accessibility of organic molecules and the enhanced CO₂ diffusion through filled pores in the pore-expanded materials.

Cyclic adsorption-desorption of pure CO₂ showed a good stability for adsorbents functionalized by grafting with DT or by impregnation with PEI, although the stability was not so good for the TEPA-impregnated material.

PEI-containing adsorbent was tested in a fixed bed of adsorption with a diluted gas mixture containing CO₂, O₂, Ar and water at 45 °C and atmospheric pressure. A noteworthy adsorption capacity of 171 mg CO₂/g was obtained, which is significantly higher than the uptake of pure CO₂ under dry conditions.

The results obtained show the potential capacity of these materials to be used at industrial scale for CO₂ capture based on TSA and VSA techniques.

References

- Aziz, B., Hedin, N., Bacsik, Z.: Quantification of chemisorption and physisorption of carbon dioxide on porous silica modified by propylamines: effect of amine density. *Micro. Microporous Mater.* **159**, 42–49 (2012)
- Barrer, R.M.: *Zeolites and Clay Minerals as Sorbents and Molecular Sieves*. Academic Press, London (1978)
- Buckingham, A.D., Disch, R.L.: The quadrupole moment of the carbon dioxide molecule. *Proc. R. Soc. London, Ser. A*, **273**, 275–289 (1963).
- Burkett, S.L., Sims, S.D., Mann, S.: Synthesis of hybrid inorganic-organic mesoporous silica by co-condensation of siloxane and organosiloxane precursors. *Chem. Commun.* **11**, 1367–1368 (1996)
- Calleja, G., Sanz, R., Arencibia, A., Sanz-Pérez, E.S.: Influence of drying conditions on amine-functionalized SBA-15 as adsorbent of CO₂. *Top. Catal.* **54**, 135–145 (2011)
- Cao, L., Man, T., Kruk, M.: Synthesis of ultra-large-pore SBA-15 silica with two-dimensional hexagonal structure using triisopropylbenzene as micelle expander. *Chem. Mater.* **21**, 1144–1153 (2009)
- Caplow, M.: Kinetics of carbamate formation and breakdown. *J. Am. Chem. Soc.* **24**, 6795–6803 (1968)
- Chen, C., Yang, S.T., Ahn, W.S., Ryoo, R.: Amine-impregnated silica monolith with hierarchical pore structure: enhancement of CO₂ capture capacity. *Chem. Commun.* **24**, 3627–3629 (2009)
- Chen, C., Son, W.J., You, K.S., Ahn, J.W., Ahn, W.S.: Carbon dioxide capture using amine-impregnated HMS having textural mesoporosity. *Chem. Eng. J.* **161**, 46–52 (2010)
- Choi, S., Drese, J.H., Jones, C.W.: Adsorbent materials for carbon dioxide capture from large anthropogenic point sources. *Chem. Sus. Chem.* **2**, 796–854 (2009)
- Fan, J., Yu, C., Lei, J., Zhang, Q., Li, T., Tu, B., Zhou, W., Zhao, D.: Low-temperature strategy to synthesize highly ordered mesoporous silicas with very large pores. *J. Am. Chem. Soc.* **127**, 10794–10795 (2005)

- Franchi, R.S., Harlick, P.J.E., Sayari, A.: Application of pore-expanded mesoporous silica. 2. Development of a high-capacity, water tolerant adsorbent for CO₂. *Ind. Eng. Chem. Res.* **44**, 8007–8013 (2005)
- Gaikwad, R., Boward, W.L., DePriest W.: Wet flue gas desulfurization technology evaluation. Project Number 11311-000. Sargent & Lundy, National Lime Association (2003).
- Harlick, P.J.E., Sayari, A.: Applications of pore-expanded mesoporous silica. 5. Triamine grafted material with exceptional CO₂ dynamic and equilibrium adsorption performance. *Ind. Eng. Chem. Res.* **46**, 446–458 (2007)
- Haynes, J.M.: *Colloid Science*, vol. 2. Chemical Society, London (1975)
- Heydari-Gorji, A., Belmabkhout, Y., Sayari, A.: Polyethylenimine-impregnated mesoporous silica: effect of amine loading and surface alkyl chains on CO₂ adsorption. *Langmuir* **27**, 12411–12416 (2011)
- Knowles, G.P., Delaney, S.W., Chaffee, A.L.: Diethylenetriamine[propyl(silyl)]-functionalized (DT) mesoporous silicas as CO₂ adsorbents. *Ind. Eng. Chem. Res.* **45**, 2626–2633 (2006)
- Leal, O., Bolívar, C., Ovalles, C., García, J.J., Espidel, Y.: Reversible adsorption of carbon dioxide on amine surface-bonded silica gel. *Inorg. Chim. Acta* **240**, 183–189 (1995)
- Lettow, J.S., Han, Y.J., Schmidt-Winkel, P., Yang, P., Zhao, D., Stucky, G.D., Ying, J.Y.: Hexagonal to mesocellular foam phase transition in polymer-templated mesoporous silicas. *Langmuir* **16**, 8291–8295 (2000)
- Lim, M.H., Stein, A.: Comparative studies of grafting and direct syntheses of inorganic-organic hybrid mesoporous materials. *Chem. Mater.* **11**, 3285–3295 (1999)
- Macquarrie, D.J.: Direct preparation of organically modified MCM-type materials. Preparation and characterisation of aminopropyl-MCM and 2-cyanoethyl-MCM. *Chem. Commun.* **16**, 1961–1962 (1996)
- Metz, B., Davidson, O., de Coninck, H., Loos, M., Meyer, L. (eds.): IPCC special report on carbon dioxide capture and storage. Cambridge Univ. Press, Cambridge, New York (2005)
- Nagarajan, R.: Solubilization of hydrocarbons and resulting aggregate shape transitions in aqueous solutions of Pluronic® (PEO-PPO-PEO) block copolymers. *Colloids Surf.* **16**, 55–72 (1999)
- Nagarajan, R., Barry, M., Ruckenstein, E.: Unusual selectivity in solubilization by block copolymer micelles. *Langmuir* **2**, 210–215 (1986)
- Namba, S., Mochizuki, A.: Effect of auxiliary chemicals on preparation of silica MCM-41. *Res. Chem. Intermed.* **24**(5), 561–570 (1998)
- Samanta, A., Zhao, A., Shimizu, G.K.H., Sarkar, P., Guota, R.: Post-combustion CO₂ capture using solid sorbents: a review. *Ind. Eng. Chem. Res.* **51**(4), 1438–1463 (2012)
- Sanz, R., Calleja, G., Arencibia, A., Sanz-Pérez, E.S.: CO₂ adsorption on branched polyethylenimine-impregnated mesoporous silica SBA-15. *Appl. Surf. Sci.* **256**, 5323–5328 (2010)
- Sanz, R., Calleja, G., Arencibia, A., Sanz-Pérez, E.S.: Amino functionalized mesostructured SBA-15 silica for CO₂ capture: exploring the relation between the adsorption capacity and the distribution of amino groups by TEM. *Micropor. Mesopor. Mater.* **158**, 309–317 (2012)
- Sing, K.S.W., Everett, D.H., Haul, R.A.W., Moscou, L., Pierotti, R.A., Rouquerol, J., Siemieniewska, T.: Reporting physisorption data for gas/solid systems with special reference to the determination of surface area and porosity (recommendations 1984). *Pure Appl. Chem.* **57**, 603–620 (1985)
- Son, W.J., Choi, J.S., Ahn, W.S.: Adsorptive removal of carbon dioxide using polyethylenimine-loaded mesoporous silica materials. *Microp. Mesop. Mater.* **113**, 31–40 (2008)
- Stein, A., Melde, B.J., Schrodin, R.C.: Hybrid inorganic-organic mesoporous silicates-nanoscope reactors coming of age. *Adv. Mater.* **12**, 1403–1419 (2000)
- Sun, J., Zhang, H., Ma, D., Chen, Y., Bao, X., Klein-Hoffmann, A., Pfänder, N., Su, D.S.: Alkanes-assisted low temperature formation of highly ordered SBA-15 with large cylindrical mesopores. *Chem. Commun.* **42**, 5343–5345 (2005)
- Tontiwachwuthikul, P., Meisen, A., Lim, C.J.: Solubility of carbon dioxide in 2-amino-2-methyl-1-propanol solutions. *J. Chem. Eng. Data* **36**, 130–133 (1991)
- US Department of Energy (DOE): Office of Science and Office of Fossil Energy: Carbon sequestration. State of science. DOE/OS-FE, Washington, DC (1999)
- van der Voort, P., Gills-D'Hamers, L., Vrancken, K.C., Vansant, E.F.: Effect of porosity on the distribution and reactivity of hydroxyl groups on the surface of silica gel. *Faraday Trans.* **87**(24), 3899–3905 (1991)
- Xu, X., Song, C., Andrésen, J.M., Miller, B.G., Scaroni, A.W.: Novel polyethylenimine-modified mesoporous molecular sieve of MCM-41 type as high-capacity adsorbent for CO₂ capture. *Energy Fuels* **16**, 1463–1469 (2002)
- Yue, M.B., Chun, Y., Cao, Y., Dong, X., Zhu, J.H.: CO₂ capture by as-prepared SBA-15 with an occluded organic template. *Adv. Funct. Mater.* **16**, 1717–1722 (2006)
- Zhao, D., Feng, J., Huo, Q., Melosh, N., Fredrikson, G.H., Chmelka, B.F., Stucky, G.D.: Triblock copolymer syntheses of mesoporous silica with periodic 50 to 300 angstrom pores. *Science* **279**, 548–552 (1998a)
- Zhao, D., Huo, Q., Feng, J., Chmelka, B.F., Stucky, G.D.: Nonionic triblock and star diblock copolymer and oligomeric surfactant syntheses of highly ordered, hydrothermally stable, mesoporous silica structures. *J. Am. Chem. Soc.* **120**, 6024–6036 (1998b).